Study of Hyperfine and Fine Interactions of Nd^{3+} and Ce^{3+} Ions in $LaNbO_4$ and $PrNbO_4$ Crystals by X-Band EPR at Liquid-Helium Temperatures†

Sushil K. Misra* and Serguei I. Andronenko

Physics Department, Concordia University, 1455 de Maisonneuve Boulevard West, Montreal, Quebec H3G 1M8, Canada

Received: June 20, 2003; In Final Form: October 2, 2003

EPR studies on diamagnetic $LaNbO_4$ and paramagnetic $PrNbO_4$ crystals doped with the Kramers ions Nd^{3+} and Ce^{3+} were carried out at X-band (9.61 GHz) in the 4−30 K temperature range. The principal values of Nd^{3+} and Ce^{3+} $\tilde{\mathbf{g}}^2$ and $\tilde{\mathbf{A}}^2$ tensors, and the orientations of their principal axes, were determined accurately from angular variations of EPR line positions recorded for rotation of the external magnetic field in three mutually perpendicular planes in the two crystals at 8 K. The larger EPR line widths of these ions in the paramagnetic $PrNbO_4$ host crystal as compared to those in diamagnetic $LaNbO_4$ are ascribed to their interaction with the host Pr^{3+} ions and presence of defects.

I. Introduction

$LaNbO_4$ single crystals doped with the Nd^{3+} ion have been investigated intensively as prospective laser materials.[1−5] Three EPR studies on $LaNbO_4$ crystals have been reported: (i) by Antipin et al.[6] on a crystal doped with Nd^{3+} ions; (ii) by Antipin et al.[7] on a crystal doped with the Kramers Ce^{3+}/Yb^{3+} ions, and (iii) by Aminov et al.[8] on a crystal doped with the non-Kramers ion Tb^{3+}. Two different sites occupied by Kramers ions were deduced in $LaNbO_4$,[6,7] based on an incorrect space symmetry ($C2$) (referred to as I2 in refs 6 and 7) of the $LaNbO_4$ crystal.[9] Subsequently, the correct space symmetry $C2/c$ (centrosymmetric) group was reported for this crystal,[10] according to which only one site is available for occupation in the unit cell by a rare earth ion.[11] The line width of the Nd^{3+} ion, 10.0 mT, reported in ref 6, was too large to enable one to discern the details of the structure of EPR lines. As well, in refs 6 and 7, the orientations of the principal axes of the $\tilde{\mathbf{A}}^2$ tensor for the Nd^{3+} ion were not specifically determined. They were assumed to be coincident with those of the $\tilde{\mathbf{g}}^2$ tensor. So far, no EPR studies on Nd^{3+} and Ce^{3+} ions in $PrNbO_4$ crystals have been reported, presumably due to their line widths being too large to observe EPR spectra. Recently, a detailed EPR study of the Gd^{3+} ion was performed on good-quality $LaNbO_4$ and $PrNbO_4$ crystals.[12] The reported increase in the Gd^{3+} EPR line width with decreasing temperature in the two crystals, implied onset of antiferromagnetic orderings consistent with the transition temperatures $T_c = 1.6$ K and $T_c = 2.4$ K in $LaNbO_4$ and $PrNbO_4$ crystals, respectively. The observed decrease in the integrated intensity of the Gd^{3+} EPR signal with lowering temperature in the two crystals was ascribed to diminution of Gd^{3+} ions due to their formation of exchange-coupled pairs with the impurity Nd^{3+} and Ce^{3+} ions present in the samples.

It is the purpose of this paper to present more detailed EPR investigations on the Nd^{3+} and Ce^{3+} ions in the crystals of diamagnetic $LaNbO_4$, than previously reported, and to present an EPR investigation of Nd^{3+} and Ce^{3+} ions in the paramagnetic $PrNbO_4$ host not previously reported. The EPR spectra were obtained for rotation of the external magnetic field (**B**) in three mutually perpendicular planes at various temperatures in the 4.2−30 K range. The EPR spectra of the Ce^{3+} and Nd^{3+} ions appear only at liquid-helium temperatures, below 25 K. The EPR line positions will be used to estimate the spin Hamiltonian parameters, that is both, $\tilde{\mathbf{g}}^2$ and $\tilde{\mathbf{A}}^2$ tensors, for the odd isotopes of Nd^{3+} which exhibit hyperfine structure, and $\tilde{\mathbf{g}}^2$ tensors for the even isotopes of Nd3+, as well as for Ce^{3+}, which do not possess any nuclear magnetic moment. The behavior of the line width and intensity of the Nd^{3+} and Ce^{3+} EPR lines in the 4−25 K temperature region, as well as that of the shape/structure of the Nd^{3+} EPR line in $LaNbO_4$ crystal will be discussed and interpreted.

II. Preparation of Samples and Crystal Structure

Synthesis of Crystals. $LaNbO_4$ and $PrNbO_4$ compounds were synthesized initially in powder form by the solid-phase reaction by mixing high-purity (99.9%) La_2O_3 or Pr_2O_3 and Nb_2O_5 compounds in stoichiometric proportions and heating at 1200 °C for 24 h. These contained trace amounts of Gd^{3+} and somewhat greater amounts of Ce^{3+} and Nd^{3+} ions as impurities. In the starting mixtures for $LaNbO_4$, 0.25 wt % of Ce_2O_3 and 0.20 wt % of Nd_2O_3 were also added. X-ray diffraction and chemical analysis were used to check the completion of the reaction, in which the compound La_3NbO_7 was first formed, which was then made to react with Nb_2O_5 at 1100 °C for 2 h, resulting in $LaNbO_4$ with about 98.5% content. Finally, the Czochralsky technique was used to grow the crystals from a melt of this powder in Ar atmosphere. For seeding, an Ir wire was rotated at 30 rpm, and withdrawn slowly from the melt at 0.5 mm/h. The dark-gray color of the single crystals, due to being grown in low oxygen partial pressure, was decolorized by annealing in oxygen atmosphere. The ingots had ca. 8 mm diameter and ca. 40 mm length. All crystals of $PrNbO_4$ grew as twinned, whereas those of $LaNbO_4$ grew both as twinned and untwinned. Both varieties of crystals of $LaNbO_4$ and $PrNbO_4$ possessed good cleavage planes, parallel to the ac crystallographic plane.

† Part of the special issue "Jack H. Freed Festschrift".

* To whom correspondence should be addressed.

10.1021/jp035758u CCC: $27.50
Published on Web 03/18/2004

Crystal Structure. The RBO_4 compounds, in which R (= La, Pr) is a rare-earth ion, and B = Nb, Ta, are isostructural with the monoclinic form of the $YTaO_4$ crystal. The space group of the $RNbO_4$ single crystal at room temperature is $C2/c$, as determined by Jeitschko et al.[10] and further confirmed by Tanaka et al.[13] The lattice parameters are[14] $a = 5.556$ Å, $b = 11.522$Å, $c = 5.204$ Å; $\beta = 94° 08'$ for $LaNbO_4$ and $a = 5.499$ Å, $b = 11.342$ Å, $c = 5.157$ Å; $\beta = 94° 57'$ for $PrNbO_4$. Confirmation of the structures of $RNbO_4$ crystals was made by Trunov et al.,[15] who also established the $C2/c$ space-group symmetry of these crystals. Due to this space-group symmetry, and because the point-group symmetry at the sites of La^{3+} and Pr^{3+} ions occupied by the rare earth impurity ions is C_2, only one set of EPR lines is expected for a rare-earth ion in an untwinned crystal $RNbO_4$. The C_2 monoclinic axis is found to be oriented perpendicular to the ac plane, the cleavage plane. The crystal transforms from the monoclinic (fergusonite) antiferroelectric phase to the tetragonal (scheelite) paraelectric phase with the space group symmetry I_1/a above the transition temperature of 495 C for $LaNbO_4$[5] and 800 C for $PrNbO_4$ single crystals.[14]

III. Experimental Results

The Nd nuclei has seven stable isotopes: ^{142}Nd, ^{143}Nd, ^{144}Nd, ^{145}Nd, ^{146}Nd, ^{148}Nd, and ^{150}Nd with natural abundances 27.13%, 12.17%, 23.80%, 8.30%, 17.18%, 5.76%, and 5.64%, respectively. The isotopes ^{144}Nd, ^{142}Nd, ^{146}Nd, ^{148}Nd, and ^{150}Nd (referred to hereafter as even isotopes) possess no nuclear magnetic moment, and therefore only one intense fine-structure EPR line is expected to be observed for them with the effective spin $S = {}^1/_2$. Each of the odd isotopes, ^{143}Nd and ^{145}Nd (referred to hereafter as odd isotopes), possesses the nuclear spin $I = {}^7/_2$; thus, eight hyperfine (hf) lines are expected to be observed for these isotopes with appropriate relative intensities in proportion to their abundances. No resolved EPR lines for these two isotopes were observed in $PrNbO_4$ due to considerable broadening of EPR lines in this paramagnetic host, unlike that in $LaNbO_4$. The Ce^{3+} ion has two isotopes ^{140}Ce and ^{142}Ce with natural abundances of 88.48% and 11.08%, respectively. They do not possess any nuclear magnetic moment; thus, in their case, only one fine-structure EPR line corresponding to the electronic spin $S = {}^1/_2$ is observed.

X-band EPR spectra of Nd^{3+}- and Ce^{3+}-doped single crystals of $LaNbO_4$ and $PrNbO_4$ were recorded in the temperature range 4−30 K on a Bruker spectrometer equipped with Oxford Instrument helium-gas flow cryostat. They were only observed at temperatures below about 25 K, shown in Figures 1 and 2 for the Nd^{3+} and Ce^{3+} ions at 8 K in untwinned $LaNbO_4$ and twinned $PrNbO_4$ crystals, respectively, for the orientation of the external magnetic field (**B**) along the magnetic Z axis. (The magnetic Z, X, and Y axes are defined to be those orientations of **B** for which extrema of the allowed, $\Delta M = \pm 1$, line positions occur; of these, the magnetic Z axis is defined to be that orientation of **B** for which maxima of EPR line positions occur, whereas the minima of the EPR line positions occur for **B** || magnetic Y axis. Here M is the electronic magnetic quantum number.) Figure 3 show the angular variations of EPR line positions for even isotopes of Nd^{3+} and those for the Ce^{3+} ion in $LaNbO_4$, at 8 K for rotation of **B** in the ZY magnetic plane. The angular variations of EPR line positions for Nd^{3+} and Ce^{3+} in $PrNbO_4$ are similar to those in $LaNbO_4$, and thus not shown here. Figure 4 show the angular variations of the hyperfine-structure line positions in $LaNbO_4$ for $^{143}Nd^{3+}$ and $^{145}Nd^{3+}$ isotopes with nonzero nuclear magnetic moments for rotation of **B** in the ZX plane. (The Gd^{3+} magnetic axes coordinate system was used as the reference frame to determine the orientations of the magnetic axes of Nd^{3+} and Ce^{3+} ions. The details of the former as deduced in ref 12 are as follows. In the untwinned $LaNbO_4$ crystal, only one set of Gd^{3+} EPR lines was observed for the two crystal components. In the twinned $LaNbO_4$ crystal, two sets of lines were observed. In the untwinned crystal, the Gd^{3+} magnetic X axis is oriented along the C_2 axis of the crystal, whereas the Z and Y axes are situated in the ac crystallographic plane. In the isostructural $YNbO_4$ crystal, Ansel'm et al.[15] considered them to be along the [101] and [10$\bar{1}$]

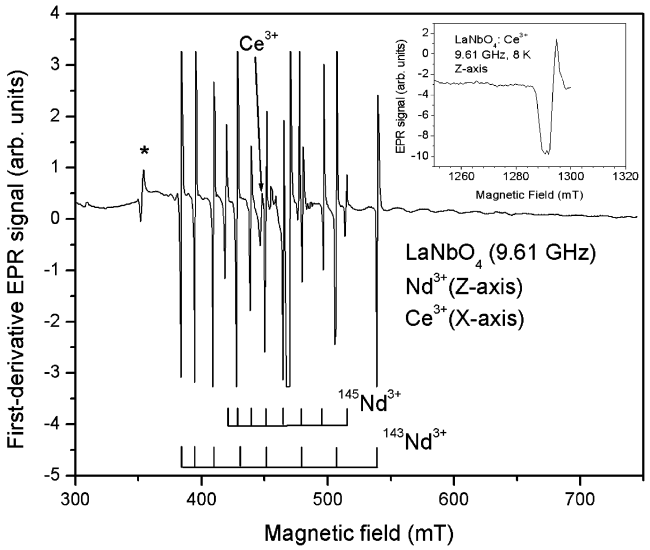

Figure 1. X-band (9.61 GHz) EPR spectrum of the Nd^{3+} ion in $LaNbO_4$ crystal at 8 K for the orientation of the external magnetic field (**B**) along the magnetic Z axis. The inset shows the EPR spectrum of the Ce^{3+} ion in $LaNbO_4$ single crystal for **B** || Z axis at 8 K. The line marked with * belongs to another unidentified ion. The Nd^{3+} Z axis is parallel to the Ce^{3+} X axis.

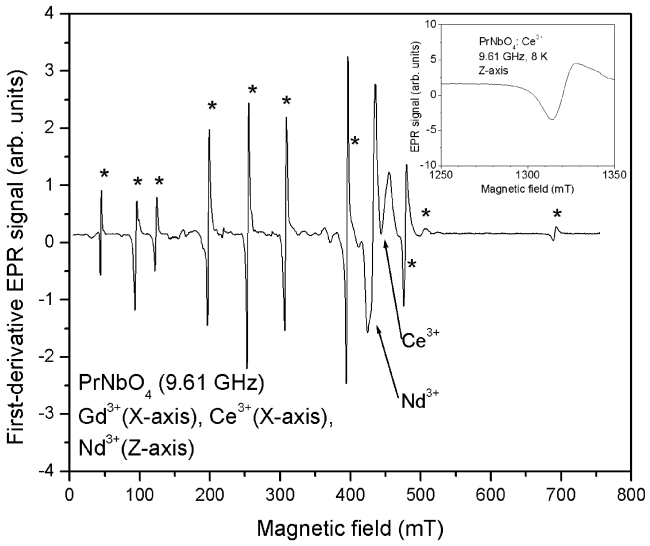

Figure 2. X-band (9.61 GHz) EPR spectrum of the Nd^{3+} ion in $PrNbO_4$ crystal (twinned) at 8 K for the orientation of the external magnetic field along the magnetic Z axis. The lines marked with an asterisk (*) belong to the Gd^{3+} ion in the twinned $PrNbO_4$ sample. For this particular orientation of **B**, the two Nd^{3+} spectra belonging to two crystals in the twinned $PrNbO_4$ sample are found to be coincident with each other. The inset shows the EPR spectrum of the Ce^{3+} ion in the $PrNbO_4$ single crystal at 8 K. The Gd^{3+} X axis, Ce^{3+} X axis, and Nd^{3+} Z axis are all parallel to each other. Due to larger line width, the hyperfine structures of Nd^{3+} lines for odd isotopes is suppressed.

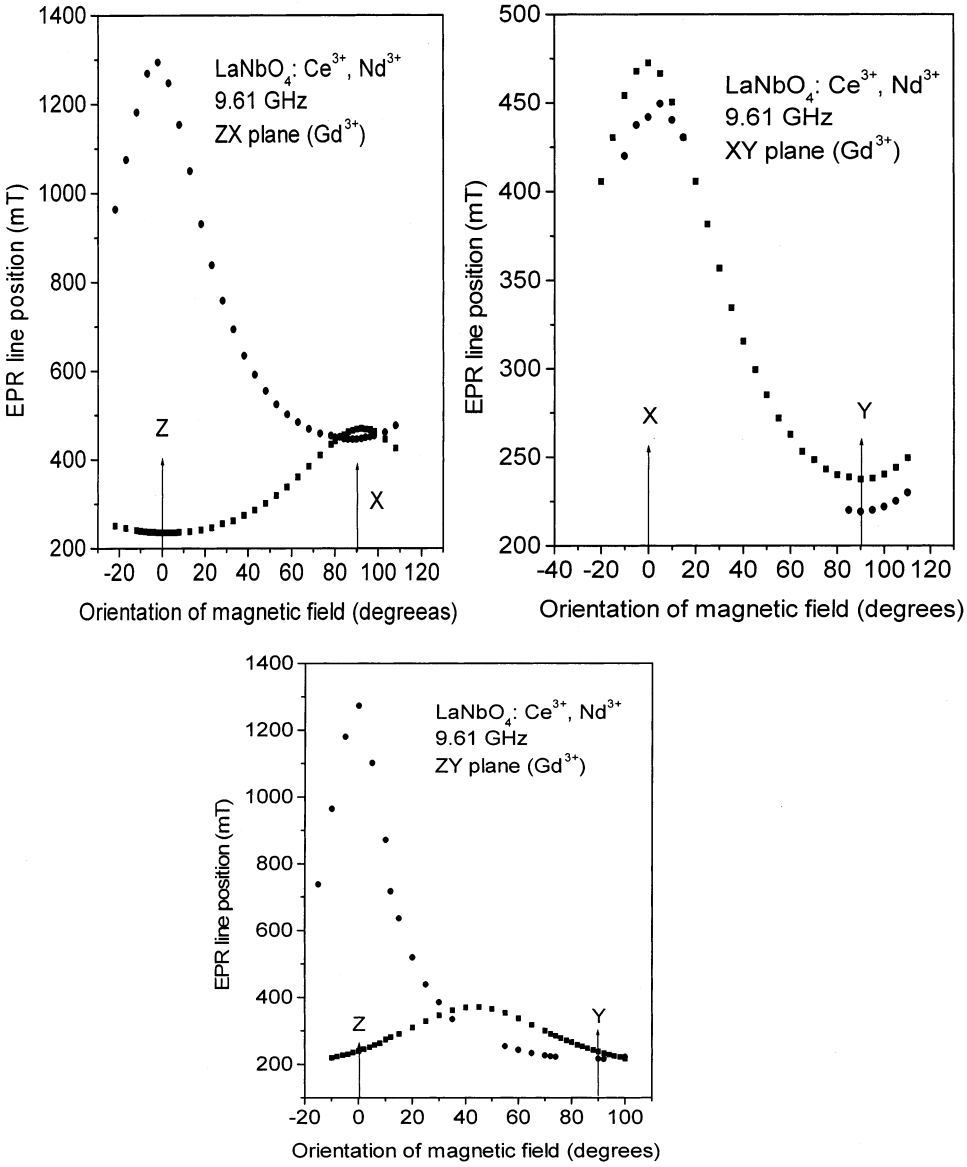

Figure 3. X-band (9.61 GHz) angular variations of Nd^{3+} and Ce^{3+} fine-structure EPR line positions for the even isotopes in $LaNbO_4$ at 8 K for the orientation of the external magnetic field in the *ZY*, *ZX*, and *XY* magnetic planes of the Gd^{3+} ion. Solid circles represent here the Ce^{3+} line positions, and squares represents the Nd^{3+} line positions.

directions. In the twinned crystal, the magnetic *X* axes of the Gd^{3+} ion for the two sets of observed EPR lines were found to be coincident, being along the 2-fold symmetry axis of the crystal, perpendicular to the cleavage plane, which is coincident with the ac plane of the crystal. Further, the two sets of the magnetic *Z* and *Y* axes were found to lie in the ac (cleavage) plane of the crystal, with the *Z* axis of one set of lines being situated 84° away from the *Z* axis of the second set of EPR lines.) The following description applies to the orientations of the magnetic axes of the various ions in the twinned crystals of both $LaNbO_4$ and $PrNbO_4$ as found here from the EPR spectra. The *Z*, *X*, and *Y* axes of the Ce^{3+} ion are coincident with those of the Gd^{3+} ion. As for the two *Z* axes of the Nd^{3+} ion, which are coincident for the two crystal components of the twinned crystal, they are found to be coincident with the *X* axis of the Gd^{3+} ion, which is parallel to the *b* axis of the crystal. The two sets of *X* and *Y* axes for the two components of the twinned crystal of the Nd^{3+} ion lie in the ac plane of the crystal, which also contains the two *Z* and *Y* axes of the Gd^{3+} ion in the twinned crystal; however, they are shifted from the respective *Z* and *Y* axes of the Gd^{3+} ion by 45°.

IV. Spin-Hamiltonian (SH) Parameters

As for the even isotopes of Nd^{3+}, as well as for the Ce^{3+} ion, there being no hyperfine (hf) interactions, the spin Hamiltonian, with spin $S = {}^1/_2$, is

$$\mathscr{H} = \mu_B \mathbf{S}\cdot\mathbf{g}\cdot\mathbf{B} \tag{1}$$

In eq 1, μ_B is the Bohr magneton and **S** is the electron spin operator.

In the presence of hf interactions, the following spin Hamiltonian with $S = {}^1/_2$ and $I = {}^7/_2$,[17] where **I** is nuclear spin operator, describes the EPR spectra for the ^{143}Nd and ^{145}Nd isotopes

$$\mathscr{H} = \mu_B \mathbf{S}\cdot\mathbf{g}\cdot\mathbf{B} + \mathbf{S}\cdot\mathbf{A}\cdot\mathbf{I} \tag{2}$$

The fine-structure line positions for the even isotopes of the

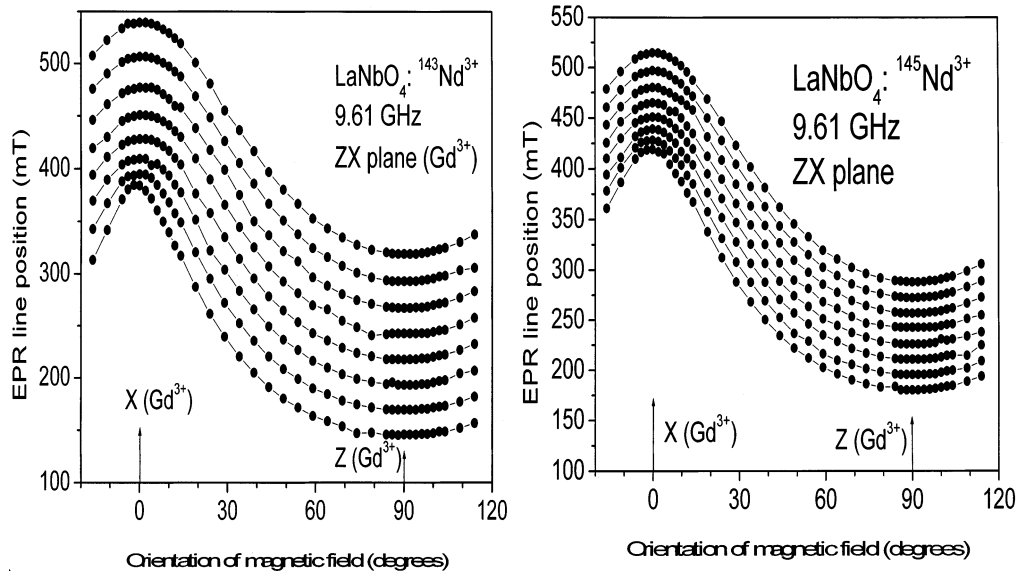

Figure 4. X-band (9.61 GHz) angular variations of $^{143}Nd^{3+}$ and $^{145}Nd^{3+}$ hyperfine line positions in $LaNbO_4$ at 8 K for the orientation of external magnetic field in the ZX magnetic plane of the Gd^{3+} ion.

TABLE 1: Principal Values of the $\tilde{g}$ and $\tilde{A}$ Matrices (Square Roots of the Principal Values of the $\tilde{g}^2$ and $\tilde{A}^2$ Tensors) for Nd^{3+} and Ce^{3+} Ions in $LaNbO_4$ and $PrNbO_4$ Crystals[a]

	$LaNbO_4$							$PrNbO_4$	
	Nd^{3+} ($S = 1/2$, $I = 0$)	$^{145}Nd^{3+}$ ($S = 1/2$, $I = 7/2$)	$^{145}Nd^{3+}$ ref 6	$^{143}Nd^{3+}$ ($S = 1/2$, $I = 7/2$)	$^{143}Nd^{3+}$ ref 6	Ce^{3+} ($S = 1/2$, $I = 0$)	Ce^{3+} ref 7	Nd^{3+} ($S = 1/2$, $I = 0$)	Ce^{3+} ($S = 1/2$, $I = 0$)
$\mathbf{g}_z$	1.460	1.474	1.46	1.495	1.46	0.534	0.53	1.592	0.510
$\mathbf{g}_x$	1.864	1.883	1.86	1.924	1.86	1.531	1.52	1.961	1.528
$\mathbf{g}_y$	3.592	3.600	3.53	3.614	3.53	3.195	3.19	3.374	3.151
$\mathbf{A}_z$ (GHz)	N/A	−0.275	0.284	−0.440	−0.465	N/A	N/A	N/A	N/A
$\mathbf{A}_x$ (GHz)	N/A	−0.362	0.360	−0.613	−0.600	N/A	N/A	N/A	N/A
$\mathbf{A}_y$ (GHz)	N/A	−0.694	0.690	−1.123	−1.124	N/A	N/A	N/A	N/A
$\mathbf{A}_J$ (GHz)		−0.137		−0.220					
n	120	960		960		66		153	119
RMSL (GHz)	0.15	0.20		0.25		0.17		0.14	0.13

[a] All values are estimated using the least-squares-fitting technique. RMSL $\equiv [\sum_j(|\Delta E_j| - h\nu)^2/n]^{1/2}$, where n is the number of lines simultaneous fitted, ΔE_j is the calculated energy differences between levels participating in resonance for the jth resonant line position, h is Planck's constant, and ν is klystron's frequency. (N/A stands for not applicable).

TABLE 2: Direction Cosines for the Principal Axes (X', Y', and Z') of the $\tilde{g}^2$ Tensor of the Even Isotopes of Nd^{3+} Ion and the Ce^{3+} Ion without Nuclear Magnetic Moments in $LaNbO_4$ and $PrNbO_4$ Crystals Relative to the Principal Axes (X, Y, and Z) of the $\tilde{g}^2$ Tensor of the Gd^{3+} Ion

		Nd^{3+}			Ce^{3+}		
		X	Y	Z	X	Y	Z
$LaNbO_4$	Z'	0.998	0.066	−0.003	0.999	0.012	0.002
	X'	−0.044	0.698	0.715	−0.012	0.999	0.036
	Y'	−0.049	0.713	−0.699	−0.016	−0.038	0.999
$PrNbO_4$	Z'	0.999	0.018	−0.019	0.999	−0.020	−0.007
	X'	0.001	0.683	0.731	0.020	0.999	−0.033
	Y'	−0.026	0.730	−0.682	0.007	0.033	0.999

TABLE 3: Direction Cosines for the Principal Axes (X', Y', and Z') of the $\tilde{g}^2$ Tensor of Odd Isotopes of Nd^{3+} Ion Relative to the Principal Axes (X, Y, and Z) of the $\tilde{g}^2$ Tensor of the Gd^{3+} Ion and Those of the $\tilde{A}^2$ Tensor (X'', Y'', and Z'') Relative to the Principal Axes (X', Y', and Z') of the $\tilde{g}^2$ Tensor of the Odd Isotopes of Nd^{3+} Ion in $LaNbO_4$ Crystal

		$\tilde{g}^2$ tensor			$\tilde{A}^2$ tensor		
		X	Y	Z	Z''	X''	Y''
$^{143}Nd^{3+}$	Z'	0.998	−0.056	0.024	0.949	0.313	0.024
	X'	0.022	0.696	0.718	−0.314	0.949	0.038
	Y'	0.058	0.716	−0.696	−0.010	−0.044	0.999
$^{145}Nd^{3+}$	Z'	0.999	−0.048	0.016	0.966	0.256	0.012
	X'	0.022	0.699	0.715	−0.257	0.966	0.041
	Y'	0.045	0.714	−0.699	−0.002	−0.042	0.999

Nd^{3+} ion and that for the Ce^{3+} ion in $LaNbO_4$ and $PrNbO_4$ at 8 K observed for various orientations of **B** in the three mutually perpendicular planes *ZX*, *ZY*, and *XY* were simultaneously fitted in the rigorous least-squares fitting procedure[18] to estimate the principal values and direction cosines with respect to the principal axes of the $\tilde{g}^2$ tensor of the Gd^{3+} ion. The estimated principal values of the $\tilde{g}^2$ tensor ($\equiv \tilde{g}^T\cdot\tilde{g}$; $\tilde{g}^T$is the transpose of the matrix $\tilde{g}$) are listed in Table 1, which also includes the parameters reported in refs 6 and 7. The corresponding orientations of the principal axes are listed in Table 2. For the odd isotopes of Nd^{3+}, the components of the anisotropic noncoincident $\tilde{g}^2$ and $\tilde{A}^2$ ($\equiv \tilde{A}^T\cdot\tilde{A}$; $\tilde{A}^T$ is the transpose of the matrix $\tilde{A}$) tensors were evaluated by fitting simultaneusly[18] all allowed hyperfine line positions ($\Delta M = \pm 1$, $\Delta m = 0$, where m is the nuclear magnetic quantum number) observed for rotation of **B** in the same three mutually perpendicular planes, as discussed above. The resulting principal values of the $\tilde{g}^2$ and $\tilde{A}^2$ tensors are listed in Table 1, whereas the direction cosines of the $\tilde{g}^2$ and $\tilde{A}^2$ principal axes are listed in Table 2.

Absolute Sign of the Hyperfine Parameters. According to Abragam and Bleaney,[17] the hyperfine parameters A_J for the

odd isotopes of Nd^{3+} possesses the negative sign, as listed in Table 1. This sign has then been used for the principal values of the $\tilde{\mathbf{A}}$ matrix listed in Table 1.

V. Discussion of Results

a. SH Parameters of Nd^{3+} and Ce^{3+} Ions in $LaNbO_4$. The parameters evaluated here can be considered to be very accurate due to a rigorous evaluation of parameters using exact eigenvalues and eigenvectors of the spin Hamiltonian matrix and fitting line positions for numerous orientations of **B** simultaneously, as compared to those reported in refs 6 and 7, included in Table 1. The principal $\tilde{\mathbf{g}}$ matrix values (square root of $\tilde{\mathbf{g}}^2$ principal values) of Ce^{3+} are found to be very close to each other in $LaNbO_4$ and $PrNbO_4$ crystals, unlike those for the Nd^{3+} ion.

b. Magnetic Axes. The data presented here have been analyzed to determine the orientations of the magnetic axes. Since, the $LaNbO_4$ crystal investigated here was untwinned, only one EPR spectrum for each of the Nd^{3+} and Ce^{3+} ions was observed, due to presence of only one magnetically inequivalent site occupied by the rare-earth ions consistent with the crystal symmetry. Since no crystallographic data are available for the orientation of the crystallographic axes, except for the orientation of the crystallographic *b* axis as determined from the morphology of the crystal, the orientations of the magnetic axes could not be determined with respect to all the three crystallographic axes only with respect to the *b* axis. Therefore, the Gd^{3+} magnetic axes were used here as reference frame.

c. EPR Line Widths. *(i) Diamagnetic Host Crystal $LaNbO_4$.* The average Nd^{3+} EPR line width is ca. 0.25 mT for the fine-structure lines for the even isotopes in the temperature range 4−10 K, whereas for the odd Nd^{3+} isotopes, the EPR line width for each hf line is ca. 0.2 mT (Figure 5). At higher temperatures, the EPR line belonging to the even isotopes broadens and splits partially into three lines, each with width to 0.4 mT. These three lines are presumably due to the three even isotopes ^{142}Nd, ^{144}Nd, and ^{146}Nd. They broaden considerably with increasing temperature, becoming totally unobservable above 20 K. However, the EPR lines due to the odd Nd isotopes with hf structure are still observable at 20 K, with the average line width being ca. 0.6 mT. From Figure 5, it is seen that the integrated intensities of the lines belonging to the various isotopes of Nd are in proportion to their relative abundances as listed in section III. The Ce^{3+} EPR line width is ca. 6.6 mT in this crystal, being independent of temperature. Here also partial splitting of this line into two is observed above 10 K, ascribed to the two isotopes of Ce^{3+} (^{140}Ce and ^{142}Ce). The Nd^{3+} EPR line width observed here is less by a factor of 40 than that reported by Antipin et al.[6] (ca. 10.0 mT). This is, probably, due to the presence of extra defects in the $LaNbO_4$ crystals used by them. The line width, ΔB, in the diamagnetic host $LaNbO_4$ is due to spin−lattice relaxation as governed by the uncertainty relation $\Delta E \Delta t = h$, where h is Plank's constant and $\Delta E \equiv g\mu_B \Delta B$ with μ_B being the Bohr magneton and Δt is related to EPR time scale.[17]

(ii) Paramagnetic Host Crystal $PrNbO_4$. The Nd^{3+} EPR line width is found to be anywhere from 2.0 to 4.0 mT for various orientations of the external magnetic field in one twinned crystal, whereas it is from 8.0 to 11.0 mT in another twinned crystal. This is due to the quality of the crystal. The Ce^{3+} EPR line width is found to be ca. 13.0 mT in a twinned crystal. For this case, there is observed no significant temperature dependence of the line width. Furthermore, the line width in this paramagnetic host crystal is much larger as compared to that in the diamagnetic host crystal $LaNbO_4$. This is caused by the magnetic interactions of the Nd^{3+} and Ce^{3+} rare-earth impurity ions with the host Pr^{3+} ions, as well as due to the influence of the indirect SHF interaction of ^{141}Pr nucleus ($I = {}^5/_2$).[19] Additional broadening of the lines is caused by the existence of numerous crystal defects in $PrNbO_4$ crystals, creating a distribution of g values. This is contrary to the behavior in the $LaNbO_4$ crystals, investigated here, which appear to be of superior quality, containing no defects.

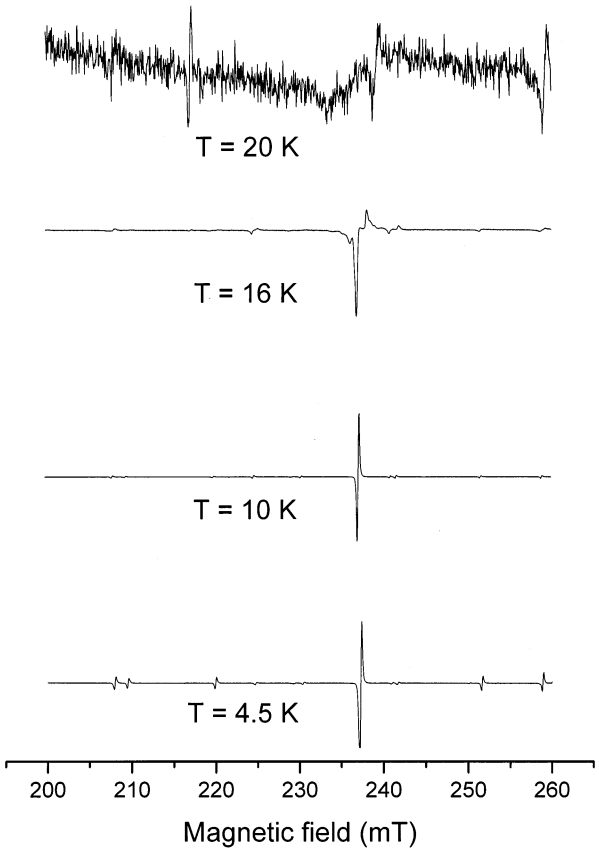

Figure 5. Temperature dependence of the Nd^{3+} EPR spectrum in $LaNbO_4$ crystal for **B** || *Z* axis of the Gd^{3+} ion.

d. Crystal Field Parameters and Wave Functions of the Ground State of Nd^{3+}. Antipin et al.[6] calculated the following wave function for the ground state of the Nd^{3+} ion in $LaNbO_4$ ($^4I_{9/2}$) with $J = 9/2$: $|\varphi\rangle = 0.686|\pm 9/2\rangle + 0.113|\pm 5/2\rangle - 0.430|\pm 1/2\rangle - 0.145|\mp 3/2\rangle + 0.587|\mp 7/2\rangle$, $|M'\rangle$ on the right-hand side being the eigenfunction of the $\mathbf{J}_z$ operator. This state is thus described predominantly by the pure doublet $|\pm 9/2\rangle$, indicating that the influence of the excited Kramers doublets is much less significant in the ground state. Then, the relation applicable to a pure doublet: $A_x/g_x = A_y/g_y = A_z/g_z = A_J/g_J$ is found to be reasonably valid for this case, as verified by the following calculation. Since, for Nd^{3+} the Landé factor is $g_J = {}^8/_{11}$,[17] the following values are calculated for the A_α/g_α ($\alpha = x, y, z$) ratios from the values listed in Table 1: $A_x/g_x = -0.192$ GHz, $A_y/g_y = -0.193$ GHz, $A_z/g_z = -0.187$ GHz; these compare favorably with $A_J/g_J = -0.188$, since $A_J = -0.137$ GHz[17] for $^{145}Nd^{3+}$. Similarly, for $^{143}Nd^{3+}$, $A_x/g_x = -0.318$ GHz, $A_y/g_y = -0.311$ GHz, $A_z/g_z = -0.294$ GHz which compare favorably with $A_J/g_J = -0.305$ GHz, since $A_J = -0.220$ GHz for this nuclear isotope.[17]

VI. Concluding Remarks

The main features of the EPR study of fine and hyperfine interactions in the ^{143}Nd and ^{145}Nd isotopes, and those of the

fine structure of the ^{142}Nd, ^{144}Nd, ^{146}Nd, ^{148}Nd, and ^{150}Nd isotopes, and the ^{140}Ce and ^{142}Ce isotopes, as reported in this paper, are as follows.

(i) More accurate values of the $\tilde{\mathbf{g}}^2$ tensor for the Ce^{3+} ion and even isotopes of the Nd^{3+} ion and the $\tilde{\mathbf{g}}^2$- and $\tilde{\mathbf{A}}^2$-tensor values for the odd isotopes of Nd^{3+} in $LaNbO_4$ were estimated in $LaNbO_4$ and $PrNbO_4$ crystals than previously reported. This was done by studying angular variation of EPR line positions in three mutually perpendicular planes, determining the orientations of the principal axes of the $\tilde{\mathbf{A}}^2$ tensor not determined previously.

(ii) The $\tilde{\mathbf{g}}^2$ tensors, and their orientations for the Nd^{3+} and Ce^{3+} ions in $PrNbO_4$ crystal, as reported here, represent a new study. The results in this paramagnetic host are analyzed to study the broadening of EPR lines as compared to those in the diamagnetic host $LaNbO_4$.

(iii) The Nd^{3+} and Ce^{3+} EPR line width are much larger, by factors of ca. 10−40 (depending on the crystal) and ca. 2 for the Nd^{3+} ion and the Ce^{3+} ion, respectively, in the paramagnetic host $PrNbO_4$ as compared to those in the diamagnetic host $LaNbO_4$. This is due to the interactions of these impurity ions with the magnetic moments of the host Pr^{3+} ions, as well as their indirect SHF interactions with nuclei of ^{141}Pr ($I = {}^5/_2$).

(iv) The EPR spectra of the even isotopes of the Nd^{3+} ion and those of the Ce^{3+} ion were observed to split partially in the temperature range 10−20 K. The splittings are ascribed to different isotopes of the impurity ions.

(v) The lowest-lying Kramers doublet for the Nd^{3+} ion in the $LaNbO_4$ crystal is found to be predominantly $|\pm 9/2\rangle$.

(vi) The two sets of magnetically inequivalent EPR spectra as observed previously[6] are explained here to be due to twinning of the $LaNbO_4$ crystal, rather than due to the wrong symmetry assumed in ref 6.

Acknowledgment. The authors are grateful to the Natural Sciences and Engineering Research Council of Canada for partial financial support. The authors thank Dr. T. Yu. Chemekova for providing the crystals.

References and Notes

(1) Kaminskii, A. A., Ed.; *Laser crystals: their physics and properties*; Springer-Verlag: New York, 1990.

(2) Kaminskii, A. A.; Fedorov, V. A.; Ngoc, C. *Inorg. Mater. (USSR)* **1978**, *14*, 1061.

(3) Godina, N. A.; Tolstoi, M. N.; Feofilov, P. P. *Opt. Spectrosc. (USSR)* **1967**, *23*, 756.

(4) Bakhshieva, G. F.; Karapetian, V. E.; Morozov, A. M.; Morozova, L. G.; Tolstoi, M. N.; Feofilov, P. P. *Opt. Spectrosc. (USSR)* **1970**, *28*, 76.

(5) Ananjeva, G. V.; Korovkin, A. M.; Kudryavtsev, A. B.; Kupchikov, A. K.; Ryskin, A. I.; Sobol, A. A. *Sov. Phys.−Solid State* **1981**, *23*, 625.

(6) Antipin, A. A.; Baikova, R. A.; Kurkin, I. N.; Shekun, L. Ya. *Sov. Phys.−Solid State* **1969**, *11*, 16.

(7) Antipin, A. A.; Baikova, R. A.; Klimaszewski, B. B.; Kurkin, I. N.; Tsvetkov, E. N.; Shlenkin, V. I. *Sov. Phys.−Solid State* **1971**, *13*, 1387.

(8) Aminov, L. K.; Ivanshin, V. A.; Kurkin, I. N. *Ferroelectrics* **1992**, *125* (1−4), 395.

(9) Komkov, A. I. *Kristallografiya (USSR)* **1959**, *4*, 836.

(10) Jeitschko, W.; Sleight, A. W.; McClellan, W. R.; Weiher, J. F. *Acta Cryst.* **1976**, *B32*, 1163.

(11) Meil'man, M. L.; Samoilovich, M. I., Eds.; *Vvedenie v EPR spektroskopiu aktivirovannuh monokristallov*; Atomizdat: Moscow, 1977 (in Russian).

(12) Misra, S. K.; Andronenko, S. I.; Chemekova, T. Yu. *Phys. Rev. B* **2003**, in press.

(13) Tanaka, M.; Saito, R.; Watanabe, D. *Acta cryst.* **1980**, *A36*, 350.

(14) Portnoi, K. I.; Timofeeva, N. I., Eds.; *Kislorodnue Soedinenia R. Z. E.*; Metallurgia: Moscow, 1986 (in Russian)

(15) Trunov, V. K.; Efremov, V. A.; Velikodnuy, Yu. A.; Averina, I. M. *Kristallografiya (Russia)* **1981**, *26*, 67.

(16) Ansel'm, L. N.; Bir, G. L.; Myl'nikova, I. E. *Sov. Phys.−Solid State*, **1971**, *12*, 1500.

(17) Abragam, A.; Bleaney, B., Eds.; *Electron Paramagnetic resonance of Transition Ions*; Clarendon: Oxford, U.K., 1970.

(18) Misra, S. K. In *Handbook of Electron Spin Resonance*; Poole, C. P., Jr., Farach, H. A., Eds.; Springer-Verlag: New York, 1999; Vol. 2, p 85.

(19) Misra, S. K.; Andronenko, S. I. *Phys. Rev. B* **2001**, *64*, 094435-(1−8).